

Resistive Wall Modes of 3D Equilibria with Multiply-connected Walls

P. Merkel, C. Nührenberg, E. Strumberger

*Max-Planck-Institut für Plasmaphysik, EURATOM Association,
D-85748 Garching*

I. Introduction

The CAS3D code solves the linear MHD stability problem for 3D equilibria in the presence of an arbitrarily shaped multiply-connected, ideal or resistive wall. For tokamak stability studies 2D codes as GATO [1], NOVA [2], CASTOR [3], MARS [4] have been widely used. They are restricted to axisymmetric wall configurations. The VALEN code [5] allows the treatment of a multiply connected wall, but the vacuum (VALEN) and plasma (DCON) contributions to the eigenmode are not computed in a fully self-consistent way.

The 3D MHD stability CAS3D code [6] was initially developed to study internal and external modes of stellarator-symmetric configurations without a conducting wall. The present generalized version can be applied to arbitrary 3D equilibria without any symmetry constraint. Two new versions of the vacuum part have been added: For a closed wall surrounding the plasma, Laplace's equation for the magnetic potential has been solved by a Fourier method. A finite element method has been applied to treat cases with multiply-connected perfectly conducting or resistive wall configurations. The paper is organized as follows. In Section II the finite element vacuum code is sketched. In Section III stability calculations are presented.

II. The Vacuum Contribution

The linear theory of ideal MHD stability can be formulated in variational form.

The contribution of the vacuum region is given by

$$W_{vac} = \frac{1}{2} \int_{S_p} df (\mathbf{n} \cdot \boldsymbol{\xi})(\mathbf{B} \cdot \mathbf{B}_0)$$

with plasma-vacuum interface S_p , displacement vector $\boldsymbol{\xi}(\mathbf{r}, t) = e^{\gamma t} \boldsymbol{\xi}(\mathbf{r})$, equilibrium magnetic field \mathbf{B}_0 , and exterior normal \mathbf{n} . The perturbed magnetic field \mathbf{B} in the vacuum region has to satisfy: $\mathbf{B} = \nabla \times \mathbf{A}$, $\nabla \times (\nabla \times \mathbf{A}) = 0$, $\nabla \cdot \mathbf{A} = 0$ with boundary conditions for \mathbf{A} in case of an ideal conducting wall

$$\mathbf{n} \times \mathbf{A} = \begin{cases} -(\mathbf{n} \cdot \boldsymbol{\xi})\mathbf{B}_0 & \text{on } S_p \text{ (plasma-vacuum interface)} \\ 0 & \text{on } S_w \text{ (conducting wall)} \end{cases}.$$

In case of a thin resistive wall the boundary condition follows from Faraday's and Ohm's law: $\nabla \times \mathbf{E} + \frac{\partial \mathbf{B}}{\partial t} = 0$, $\boldsymbol{\sigma} \mathbf{E} = \mathbf{J}$. Assuming that the perturbed quantities vary as $e^{\gamma t}$ one gets with \mathbf{j}_w the current on the resistive wall, $\boldsymbol{\sigma}$ the conductivity and d the wall thickness

$$\mathbf{n} \cdot (\nabla \times \mathbf{j}_w) = -\boldsymbol{\sigma} d \gamma \mathbf{n} \cdot \mathbf{B} \quad \text{on } S_w \text{ (resistive wall)}.$$

The vector potential \mathbf{A} can be generated by surface currents $\mathbf{j}_p, \mathbf{j}_w$ on the plasma-vacuum interface and the conducting wall:

$$\mathbf{A} = \frac{1}{4\pi} \int_{S_p} df' \frac{\mathbf{j}'_p}{|\mathbf{x} - \mathbf{x}'|} + \frac{1}{4\pi} \int_{S_w} df' \frac{\mathbf{j}'_w}{|\mathbf{x} - \mathbf{x}'|}.$$

The surface-currents have to be determined such that the boundary conditions for \mathbf{A} on S_w and S_p are fulfilled. For a finite element problem it is advantageous to use a variational method. One introduces the functional [7]

$$\begin{aligned} \mathcal{L} = & \frac{1}{8\pi} \int_{S_p} df \int_{S_p} df' \frac{\mathbf{j}_p \cdot \mathbf{j}'_p}{|\mathbf{x}_p - \mathbf{x}'_p|} + \frac{1}{4\pi} \int_{S_p} df \int_{S_w} df' \frac{\mathbf{j}_p \cdot \mathbf{j}'_w}{|\mathbf{x}_p - \mathbf{x}'_w|} \\ & + \frac{1}{8\pi} \int_{S_w} df \int_{S_w} df' \frac{\mathbf{j}_w \cdot \mathbf{j}'_w}{|\mathbf{x}_w - \mathbf{x}'_w|} + \int_{S_p} df' \mathbf{j}_p \cdot \mathbf{A}_{ext} + \frac{1}{2\sigma d\gamma} \int_{S_w} df' \mathbf{j}_w \cdot \mathbf{j}_w \end{aligned}$$

where $\mathbf{n} \times \mathbf{A}_{ext} = (\mathbf{n} \cdot \boldsymbol{\xi}) \mathbf{B}_0$, $\mathbf{B}_0 = \nabla s \times \nabla (F'_p v - F'_T u)$ and u, v are magnetic coordinates.

An ansatz for a divergence-free surface current is given by $\mathbf{j}_p = \mathbf{n} \times \nabla \phi_p$, $\mathbf{j}_w = \mathbf{n} \times \nabla \phi_w$, where ϕ_p, ϕ_w are current-potentials. A general Ansatz for ϕ_p is given by

$$\phi_p = J_p u + I_p v + \phi_p^*(\mathbf{x}(u, v)),$$

where $\phi_p^*(\mathbf{x}(u, v))$ is a single-valued function. The secular terms with the net-toroidal(net-poloidal) currents $J_p, (I_p)$ play a role only for the $m = 0, n = 0$ mode.

Varying \mathcal{L} with respect to ϕ_p and ϕ_w one obtains the above given boundary conditions.

For the finite element procedure the surfaces are discretized into triangles:

$$\mathbf{x} = \alpha \mathbf{x}_1 + \beta \mathbf{x}_2 + \gamma \mathbf{x}_3, \quad 0 < \alpha + \beta + \gamma < 1, \quad \mathbf{x}_{ik} = \mathbf{x}_i - \mathbf{x}_k, \quad i, k = 1, 2, 3$$

The current density \mathbf{j}_Δ on each triangle is assumed to be constant:

$$\mathbf{j}_\Delta = \frac{\phi_1 \mathbf{x}_{23} + \phi_2 \mathbf{x}_{31} + \phi_3 \mathbf{x}_{12}}{|\mathbf{x}_{21} \times \mathbf{x}_{32}|}$$

where the ϕ_i are the values of the current potential at the vertices of the triangle.

Varying the discretized \mathcal{L} with respect to the ϕ_i one gets a set of linear equations for the ϕ_i .

With the Fourier expansions of the normal component of $\boldsymbol{\xi}$: $\xi^s = \boldsymbol{\xi} \cdot \nabla s$ and ϕ_p

$$\xi^s = \sum_{m,n} \hat{\xi}_{mn}^s \sin 2\pi(mu + nv) + \hat{\xi}_{mn}^c \cos 2\pi(mu + nv),$$

the vacuum matrix can be written as

$$W_{vac} = 2\pi^2 \sum_{m,n,m',n'} (nF'_T + mF'_p) (\hat{\xi}_{mn}^s, \hat{\xi}_{mn}^c) \begin{pmatrix} W_{mn,m'n'}^{ss} & W_{mn,m'n'}^{sc} \\ W_{mn,m'n'}^{cs} & W_{mn,m'n'}^{cc} \end{pmatrix} \begin{pmatrix} \hat{\xi}_{m'n'}^s \\ \hat{\xi}_{m'n'}^c \end{pmatrix} (n'F'_T + m'F'_p)$$

$$W_{mn,m'n'}^{ss} = \int_{S_p} dudv \cos 2\pi(mu + nv) \left(\int_{S_p} \phi_p^{*s}(\mathbf{x}')_{m'n'} \frac{(\mathbf{x}_p - \mathbf{x}'_p) \cdot d\mathbf{f}'}{|\mathbf{x}_p - \mathbf{x}'_p|^3} + \int_{S_w} \phi_w^{*s}(\mathbf{x}')_{m'n'} \frac{(\mathbf{x}_p - \mathbf{x}'_w) \cdot d\mathbf{f}'}{|\mathbf{x}_p - \mathbf{x}'_w|^3} \right)$$

where the $\phi_p^{*s}(\mathbf{x})_{mn}, \phi_w^{*s}(\mathbf{x})_{mn}$ are the contributions to ϕ_p^*, ϕ_w^* produced by the harmonic $\hat{\xi}_{mn}^s$.

III. Applications

The equilibria of all examples presented are calculated with the VMEC code [8,9]. For an ASDEX-Upgrade type equilibrium (see Fig.1a-b) with a perfectly conducting closed wall the growth rates of a $n = 1$ external kink mode have been computed.

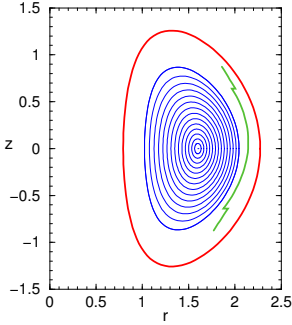


Fig.1a

Fig.1a-b Flux-surfaces, q-profile and pressure of an ASDEX-Upgrade type equilibrium: $\langle \beta \rangle = 0.05$

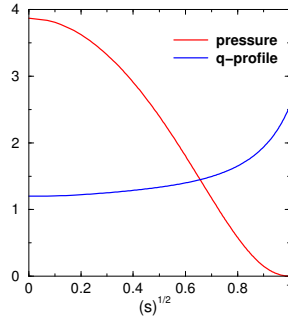


Fig.1b

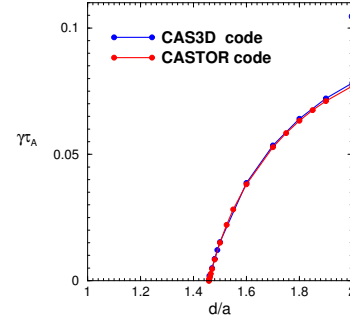


Fig.2 Growth rates of an external kink mode versus plasma-wall distance

In Fig.2 the growth rates are plotted versus the plasma-wall distance b/a ($a =$ plasma radius, $b =$ wall radius). The equilibrium is stable for values $b/a < 1.45$ of the ideal conducting wall. For a resistive wall at $b/a = 1.2$ growth rates of the external kink mode versus the wall-resistance $1/(\sigma d)$ are shown in Fig.3. The results are compared with those obtained with the 2D CASTOR_FLOW code- an extended version of the 2D CASTOR code - and show excellent agreement.

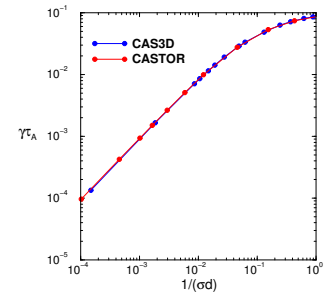


Fig.3 Growth rates of the $n = 1$ resistive wall mode

For a preliminary design of a multiply-connected wall (Fig.4) for ASDEX-Upgrade the stabilization of the $n = 1$ kink mode has been studied for the equilibrium shown in Fig.1 but with $\langle \beta \rangle = .03$. For $\sigma = \infty$ the mode is stabilized by the wall sufficiently close to the plasma (see green wall in Fig.1). For $\sigma \neq \infty$ the mode appears on the resistive time scale. Growth rates versus resistance $1/(\sigma d)$ are plotted in Fig.5. In Fig.6a the m-harmonics of ξ^s of the $n = 1$ kink mode for the case without wall are shown and in Fig.6b for the case with resistive wall.

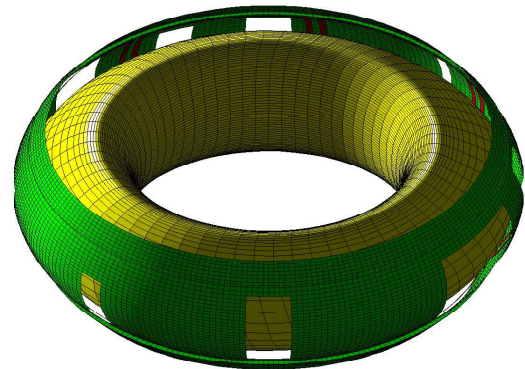


Fig.4 Preliminary design of a stabilizing wall for ASDEX-Upgrade

The kink unstable quasi-axisymmetric equilibrium [10] shown in Fig.7 can be stabilized by a perfectly conducting ($\sigma = \infty$) closed wall at $b/a = 1.3$. For a wall with $\sigma \neq \infty$ one gets a resistive wall mode. The growth rates versus resistance $1/(\sigma d)$ are shown in Fig.8. The structure of the most unstable mode changes with decreasing resistivity. For high resistivity the $(m,n) = (2,1)$ -harmonic with even parity dominates (Fig.9a) for low resistivity the $(m,n) = (5,3)$ -harmonic with odd parity (Fig.9b).

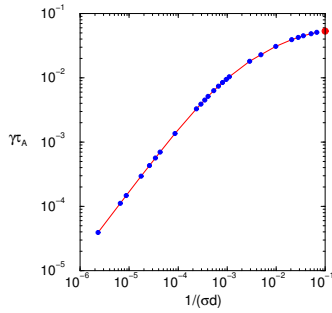


Fig.5 Growth rates of the $n = 1$ resistive wall mode for the wall shown in Fig.4

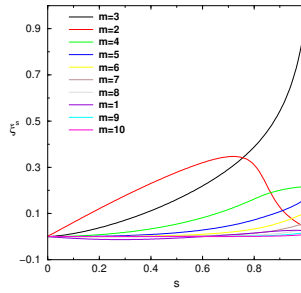


Fig.6a

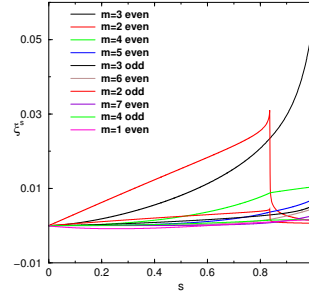


Fig.6b

Fig.6a-b m harmonics of ξ^s for the $n = 1$ external kink mode: a) without wall, b) with resistive wall $1/(\sigma d) = 2.3 \times 10^{-6}$

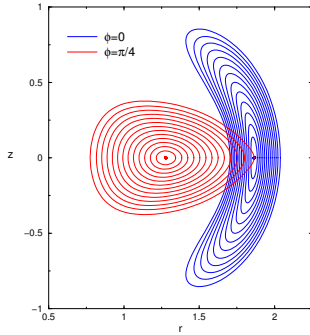


Fig.7a

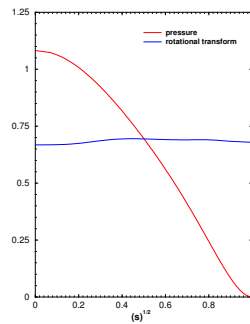


Fig.7b

Fig.7a-b flux-surfaces (a), rotational transform (b), pressure(b) of a quasi-axisymmetric equilibrium with $\langle \beta \rangle = 0.013$, $B_0 = .9$ T, current $I = 280$ kA

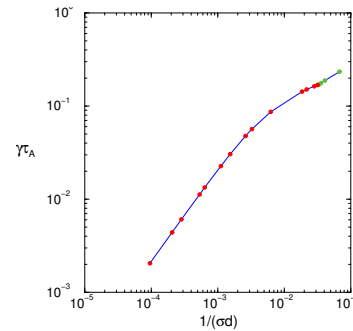


Fig.8 Growth rates of a resistive wall mode for a quasi-axisymmetric equilibrium

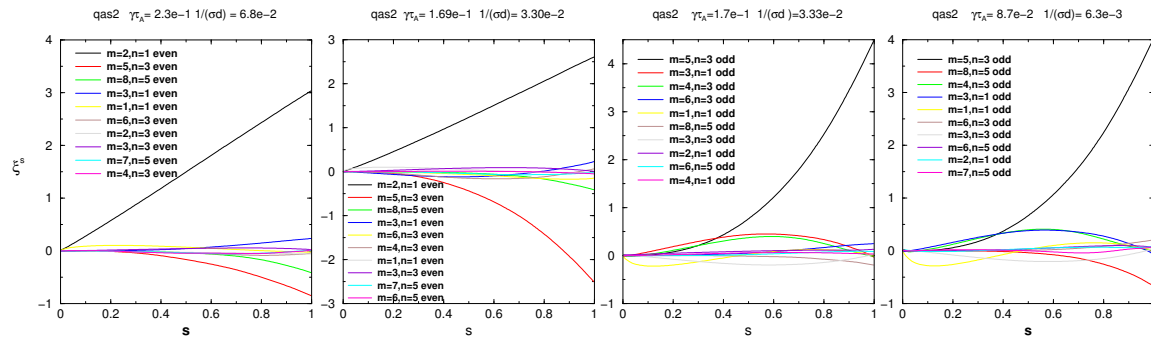


Fig.9 sequence of eigenfunctions: (m,n) -harmonics of ξ^s are shown for decreasing resistance: dominant external mode changes from $(m,n) = (2, 1)$ to $(m,n) = (5, 3)$

References

- [1] L.C. Bernard et al., Comput. Phys. Comm. **24** (1981) 143.
- [2] D.J. Ward et al., J. Comput. Phys. **104** (1993) 221
- [3] W. Kerner et al., J. Comput. Phys. **142** (1998) 271
- [4] A. Bondeson et al, Nucl. Fusion **41** (2001) 455
- [5] J. Bialek et al., Phys. Plasmas **8** (2001) 2170
- [6] C. Schwab, Phys. Fluids **B5** (1993) 3195, C. Nührenberg, Phys. Plasmas **3** (1996) 2401
- [7] S.W.Haney, J.P.Freidberg, Phys. Fluids **B5** (1989) 3195
- [8] S.P. Hirshman et al., Phys. Fluids **28** (1985) 1387,
- [9] S.P. Hirshman et al, Comput. Phys. Comm. **43** (1986) 143
- [10] S. Okamura et al, Nucl.Fusion **41** (2001) 1865